Nonextensivity of the cyclic lattice Lotka-Volterra model

G. A. Tsekouras,[1,2] A. Provata,[1,*] and C. Tsallis[3,†]
[1]*Institute of Physical Chemistry, National Research Center "Demokritos," 15310 Athens, Greece*
[2]*Department of Physics, University of Athens, 10679 Athens, Greece*
[3]*Centro Brasileiro de Pesquisas Fisicas, Rua Xavier Sigaud 150, 22290-180 Rio de Janeiro, Brazil*
(Received 12 February 2003; revised manuscript received 9 September 2003; published 30 January 2004)

We numerically show that the lattice Lotka-Volterra model, when realized on a square lattice support, gives rise to a *finite* production, per unit time, of the nonextensive entropy $S_q=(1-\Sigma_i p_i^q)/(q-1)$ ($S_1=-\Sigma_i p_i \ln p_i$). This finiteness only occurs for $q=0.5$ for the $d=2$ growth mode (growing droplet), and for $q=0$ for the $d=1$ one (growing stripe). This strong evidence of nonextensivity is consistent with the spontaneous emergence of local domains of identical particles with fractal boundaries and competing interactions. Such direct evidence is, to our knowledge, exhibited for the first time for a many-body system which, at the mean field level, is conservative.

DOI: 10.1103/PhysRevE.69.016120 PACS number(s): 05.10.Ln, 05.65.+b, 05.40.−a

I. INTRODUCTION

Many natural and artificial systems are known today to be hardly, or not at all, tractable within Boltzmann-Gibbs statistical mechanics, hence the usual thermodynamics. Such is the case of systems which include long-range interactions or long-range microscopic (or mesoscopic) memory, or other sources of (multi)fractality. Phenomena where many spatial and/or temporal scales are involved typically exhibit power laws. The celebrated Boltzmann-Gibbs (BG) entropy $S_{BG}=-\Sigma_i p_i \ln p_i$ appears to be inadequate for handling the thermostatistics associated with such situations. This is due to the fact that the corresponding stationary states do *not* emerge through ergodic dynamics. An ubiquitous class of the above anomalous systems has nonlinear dynamics which generate *weak* chaos, in the sense that the sensitivity to the initial conditions is less than exponential in time. Such situations quite naturally accommodate with an entropy which generalizes the BG one, namely,

$$S_q=\frac{1-\sum_i p_i^q}{q-1}\ (q\in\mathbb{R};S_1=S_{BG}). \tag{1}$$

For independent systems A and B (i.e., such that $p_{ij}^{A+B}=p_i^A p_j^B$), this entropy satisfies $S_q(A+B)=S_q(A)+S_q(B)+(1-q)S_q(A)S_q(B)$. It is due to this property of nonextensivity that the thermostatistical formalism based on Eq. (1) is usually referred to as nonextensive statistical mechanics [1] (see Ref. [2] for recent reviews). This theory has received many applications in areas such as self-gravitating polytropes [3], electron-positron annihilation [4], turbulence [5], motion of *Hydra viridissima* [6], anomalous diffusion [7,8], classical [9] and quantum [10] chaos, long-range-interacting many-body Hamiltonians [11], option pricing [12], particular biological processes involving a large number of degrees of freedom [13,14], among others.

The original Lotka-Volterra (LV) model was first introduced in population dynamics to study predator-prey systems [15–17]. Many variants of this model followed with applications in diverse fields, such as ecology, sociology, economy, and chemistry. While the original LV model was introduced as a mean-field (MF) scheme, the variants include lattice gas [18–21], reaction-diffusion [22], and stochastic models [23,24]. The lattice Lotka-Volterra (LLV) model [25,26] with cyclic interactions amongst a number of species has been studied as a modification to the original LV model at the MF level. Implementations of the LLV model on one-dimensional (1D) lattice with variable number of species has manifested distinct non-MF behavior [26]. On higher dimensions the LLV has exhibited stationary patterns [27,28], spatial clustering [25], fractality [29], and dynamical pattern formation [30].

Since fractality often accompanies nonextensivity, it is natural to pose the question whether the LLV model is indeed consistent with the nonextensive premises. The aim of the present paper is to verify that this model can be characterized within the extended thermostatistics with $q\neq 1$. In particular we study the LLV model with various initial conditions, namely, at (a) the domain formation mode, (b) the nucleus (or droplet) growth mode, (c) the stripe growth mode, and (d) the roughening mode. Modes (b) and (c) enable, as we shall see, the direct calculation of q. Several analytical or numerical calculations of q exist already in the literature, but this is the first time, to our knowledge, such evidence is directly provided, through the time evolution of S_q itself, on a many-body system which is conservative at the MF level.

II. THE LATTICE LOTKA-VOLTERRA MODEL ON SQUARE LATTICE

The LLV model is a minimal complexity model, with MF conservative dynamics which can be directly implemented on lattice and involves only two reactive species X_1 and X_2 (adsorbed on a lattice support) and the empty sites of the

*Electronic address: aprovata@limnos.chem.demokritos.gr
†Electronic address: tsallis@cbpf.br

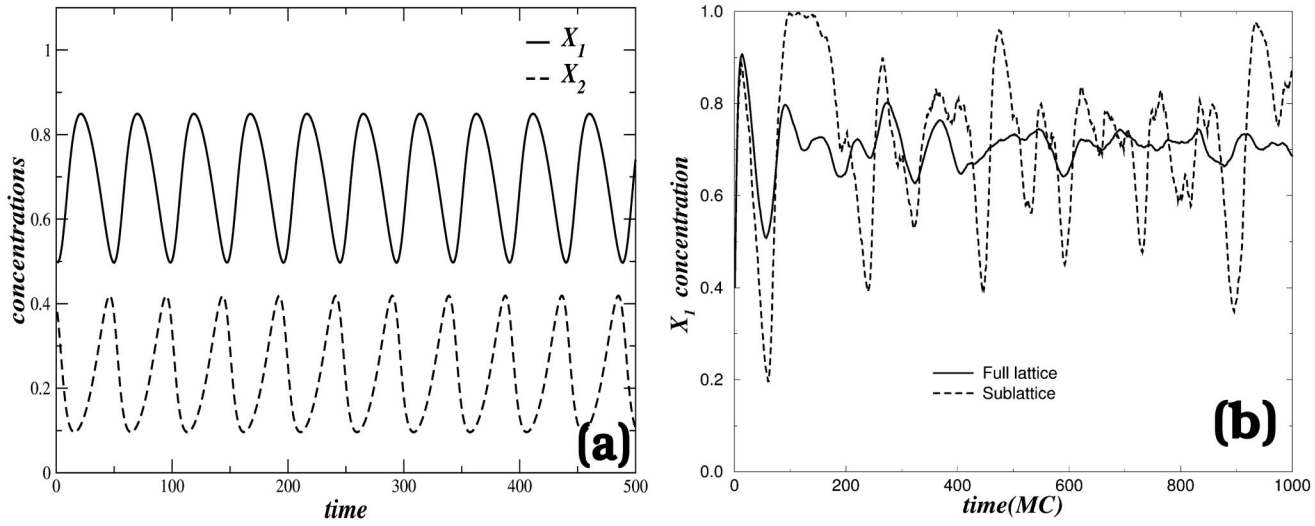

FIG. 1. (a) The mean-field approximation concentrations $x_1(t)$ and $x_2(t)$ for $(x_1(0),x_2(0),s(0))=(0.5,0.4,0.1)$ and $(k_1,k_2,k_s)=(0.9,0.3,0.1)$. (b) Monte Carlo simulations; the solid (dotted) line corresponds to $x_1(t)$ over the full lattice (sublattice).

support S. All reactive steps are bimolecular and the reaction occurs via hard core interactions. Schematically, the LLV model has the following form [25]:

$$X_1+X_2 \xrightarrow{k_s} 2X_2, \tag{2a}$$

$$X_2+S \xrightarrow{k_1} 2S, \tag{2b}$$

$$S+X_1 \xrightarrow{k_2} 2X_1. \tag{2c}$$

In particular, a particle X_1 adsorbed on a lattice site changes its state into X_2 when it is found in the neighborhood of another X_2 particle. The step (2a) is an autocatalytic reactive step. A particle X_2 desorbs leaving an empty site S, if in the neighborhood another empty site S is found. The step (2b) is a cooperative desorption step. Finally, a particle X_1 can be adsorbed on an empty lattice site S if in the neighborhood another X_1 particle is found. The step (2c) is a cooperative adsorption step. In a predator-prey system species X_1 may represent the prey, species X_2 represents the predator, while S represents empty space which can be occupied by either predator or prey during the evolution.

We now recall briefly some of the mean-field and lattice properties of the LLV, which have been studied in detail in previous works [25,29].

In the MF approximation the LLV model, Eqs. (1), can be described via the kinetic rate equations:

$$\frac{dx_1}{dt}=x_1(-k_sx_2+k_2s), \tag{3a}$$

$$\frac{dx_2}{dt}=x_2(k_sx_1-k_1s), \tag{3b}$$

$$\frac{ds}{dt}=s(-k_2x_1+k_1x_2), \tag{3c}$$

where x_1, x_2, and s correspond to the mean coverage of the lattice with particles X_1, X_2 and empty sites S, respectively. In Eqs. (3), the mean coverages satisfy identically the conservation condition $x_1+x_2+s=C$, where C is a constant which can be chosen equal to unity, corresponding to interpreting x_1, x_2, and s as fractions of the overall lattice, respectively, occupied by X_1 particles, X_2 particles, or being empty. Using $C=1$ it is possible to eliminate one of the three variables, say $s=1-x_1-x_2$, and to reduce system (3) to two equations. This reduced system admits four steady state solutions, three of which are trivial and one nontrivial [25]; namely, with $K=k_1+k_2+k_3$,

$$x_{1s}=0,\ x_{2s}=0 \quad \text{(empty lattice)}, \tag{4a}$$

$$x_{1s}=1,\ x_{2s}=0 \quad \text{(lattice poisoned by } X_1\text{)}, \tag{4b}$$

$$x_{1s}=0,\ x_{2s}=1 \quad \text{(lattice poisoned by } X_2\text{)}, \tag{4c}$$

$$x_{1s}=k_1/K,\ x_{2s}=k_2/K \quad \text{(nontrivial state)}. \tag{4d}$$

A linear stability analysis shows that the trivial states are saddle points while the nontrivial one is a center compatible with an additional constant of motion $C'=x_1^{k_1}x_2^{k_2}(1-x_1-x_2)^{k_s}$ [31,32] at the MF level. Figure 1(a) depicts the temporal evolution of the system for typical values of (k_1,k_2,k_s) and initial conditions. The black solid line represents the concentration of X_1 and the dashed line the concentration of X_2. The motion is periodic but nonharmonic. The amplitude of the periodic motion, for given parameter values, depends solely on the initial conditions [25,29]. At this level of description the system size does not enter into the calculations since the MF approximation involves only average concentrations.

To mesoscopically describe the system on a lattice, many details enter: lattice size and geometry, number of nearest neighbors (coordination number), interaction range, etc. To

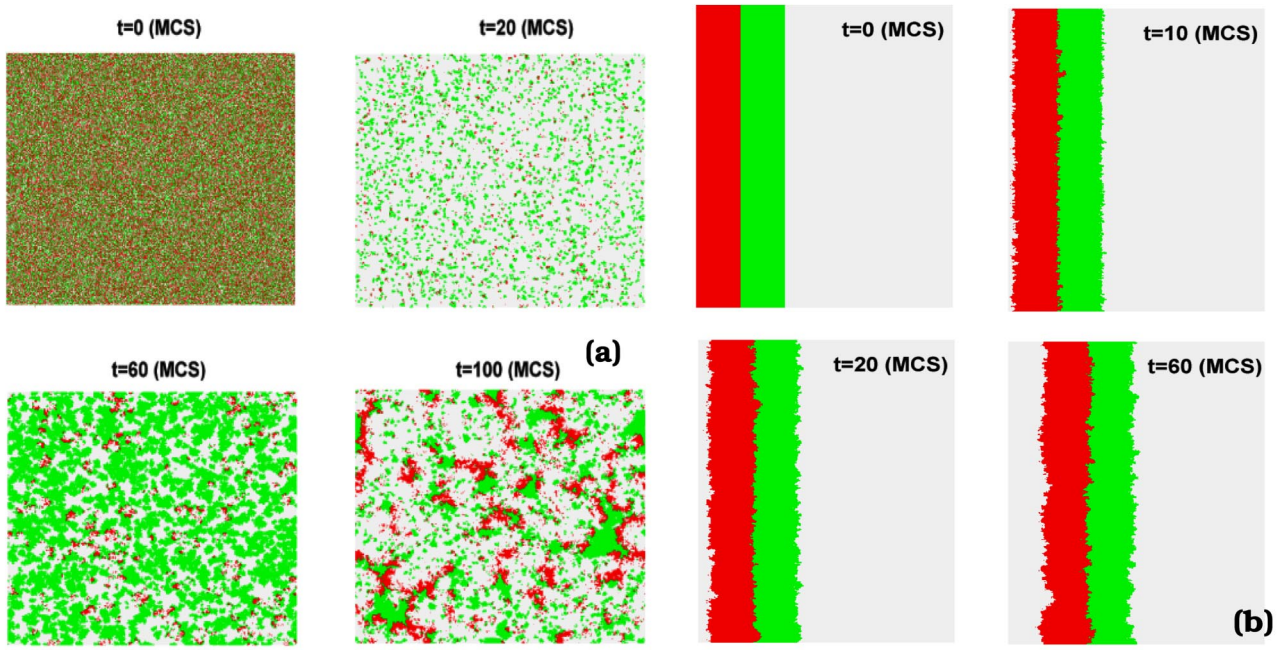

FIG. 2. (a) Four different snapshots during the evolution of LLV for random uniform initial conditions (i.e., $p_i=(l/L)^2$, hence $S_q(t=0)=[(L/l)^{2(1-q)}-1]/(1-q)$, where l is the size of the nonoverlapping windows) on a $L=500$ square lattice at the "domain formation mode"; $(k_1,k_2,k_s)=(0.9,0.3,0.1)$. (b) Four different snapshots during the evolution of LLV starting from initial conditions containing stripes of identical particles at the "roughening mode"; $(k_1,k_2,k_s)=(1.0,1.0,1.0)$.

realize the square lattice LLV we adopt a typical Kinetic Monte Carlo (KMC) algorithm (details in Refs. [25,29]), which is as follows.

(1) At every microscopic step one lattice site is randomly chosen.

(2) One of the nearest neighbors is also selected randomly.

(3) If the original chosen site is X_1 (X_2) and the selected neighbor is X_2 (S) then the chosen site changes to X_2 (S) with probability $k_s(k_1)$; if the original chosen site is S and the selected neighbor is X_1 then the chosen site changes to X_1 with probability k_2; otherwise the system remains as it is.

(4) Return to step (1).

In the KMC procedure the unit of time is chosen as $1/N$, where N is the total number of lattice sites (occupied and empty). For example, for square lattice, $N=L^2$, where L is the linear size of the lattice. With this choice of microtime, in one Monte Carlo step (MCS) all lattice sites are, on an average, scanned once. In Fig. 1(b) typical behavior of the temporal evolution of the KMC concentrations is shown. In particular, the concentrations of X_1 is depicted on the full lattice of size $L\times L=2^8\times 2^8$ (solid line) and on a sublattice of size $l\times l=2^5\times 2^5$ (dotted line). Periodic boundary conditions are used in all simulations. It is clear that while on the sublattice the concentrations show oscillatory behavior with added noise, on the entire lattice the oscillations shrink.

Figures 2(a) and 2(b) show typical evolutions of the LLV system starting from different initial conditions [Figs. 2(a) and 2(b) at $t=0$]. In Fig. 2(a) initially the system is a homogeneous lattice with equal concentrations of X_1,X_2 particles and empty sites S. As time increases the system develops local domains and each domain behaves as a local oscillator with specific characteristic frequency. Because the various domains have different phases, globally, no oscillations are observed, in contrast with the MF predictions [25]. Moreover, it has been shown [29] that the different species organize in local domains which present competing interactions and have fractal boundaries. In this figure and hereafter the X_1 particles are depicted in green (gray) color, the X_2 in red (black), and the empty sites in white. The fractal properties of the spatial structures can be used to measure the size of the local oscillators [29] and point out to a nonextensive formalism for the calculation of its entropy. Similarly, in Fig. 2(b) we present the dynamical evolution of the LLV system at the "roughening mode," where initially a flat interface separates two stripes of identical particles. The setup of the system at the initial state contains one stripe of size $S\times L=50\times 500$ consisting only of X_1 particles followed by a stripe of the same size but consisting only of X_2 particles, while the rest of the lattice is covered by S, see Fig. 2(b) at $t=0$. As time increases, the originally flat interfaces roughen and the stripes are deformed. The process is dynamical and all interfaces move to the right with the same average velocity. In Fig. 2(b) while the size of the stripes is on the average kept constant, fluctuations make their shape vary significantly. In fact, after sufficiently long times (depending on the width S and the size L of the stripes) the stripes will mix and the typical fractal patterns of Fig. 2(a) will reappear. These two examples and the ones which will be presented in the sequel demonstrate the rich complex LLV structures which give rise to nonextensive entropy production.

III. ENTROPY CALCULATIONS

To describe the temporal evolution of the entropy with respect to one of the species, e.g., X_1, we start from a given

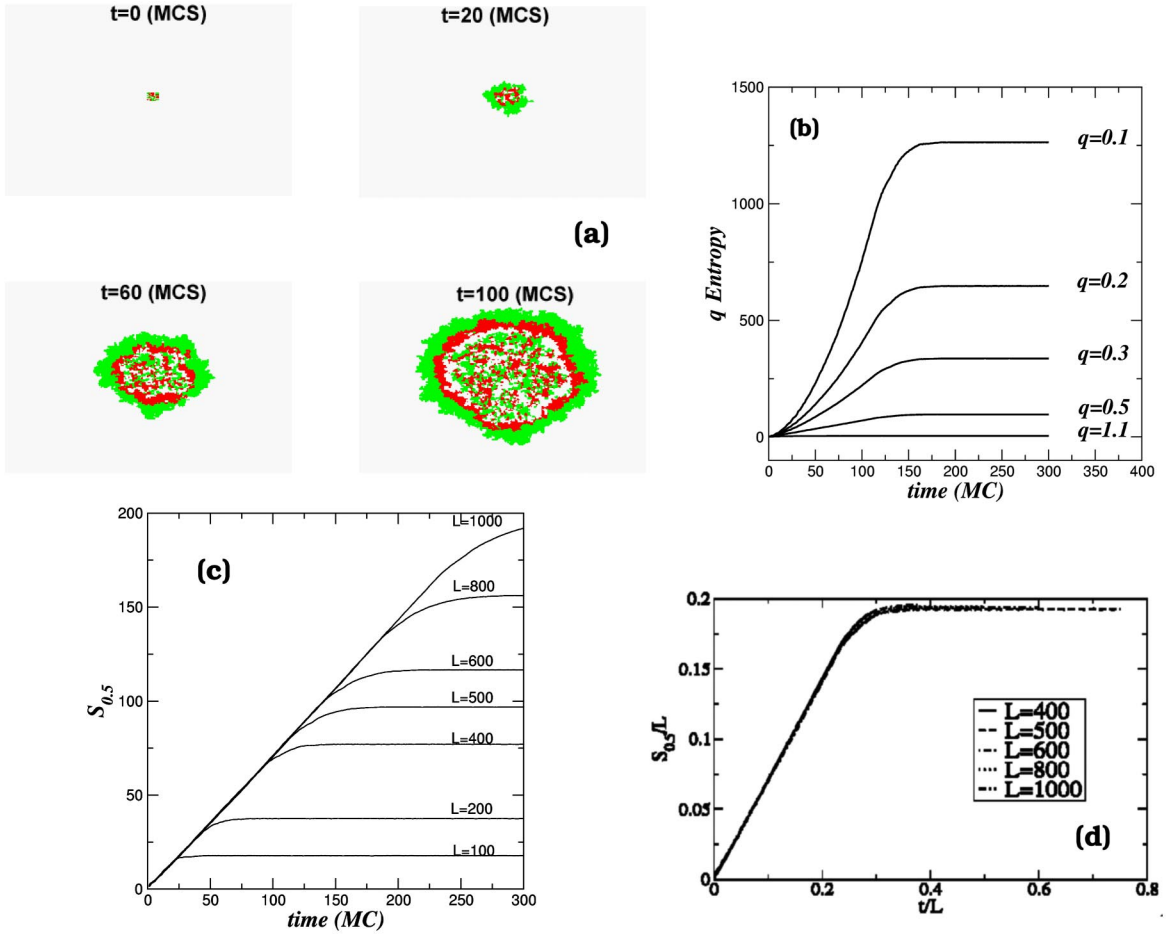

FIG. 3. (a) Four different snapshots during the evolution of a system covered initially by S with one small mixed droplet. The system linear size is $L=500$ while the droplet size is $l=8$; $(k_1,k_2,k_s)=(1.0,1.0,1.0)$. (b) $S_q(t)$. (c) $S_{0.5}(t)$ for various lattice sizes. (d) Collapse of the (c) data.

configuration, with specific initial conditions on lattice and let the system evolve according to the KMC algorithm. The choice of the particular species does not play any role in the entropy calculations, since the model is cyclic and all the species are equivalent. As time increases the system passes through various configurations which we record at regular temporal intervals. Let us call $C(t)=\{C_{ij}(t)\}$, $i=1,\ldots,L; j=1,\ldots,L$ the specific configuration of the lattice at time t, while $C_{ij}(t)$ denotes the state of site (i,j) at time t; namely,

$$C_{ij}=\begin{cases}1 & \text{if site } (i,j) \text{ is occupied by } X_1\\ -1 & \text{if site } (i,j) \text{ is occupied by } X_2\\ 0 & \text{if site } (i,j) \text{ is occupied by } S.\end{cases}$$

Within each configuration we introduce a set of M nonoverlapping windows $\{W_i\}$ $(i=1,\ldots,M)$ of size $l\times l$ which cover completely the lattice. The number of windows is $M=n^2=(L/l)^2$. Consequently

$$C(t)=\bigcup_{i=1}^{M} W_i. \tag{5}$$

Let us denote with p_i the probability that window i is occupied by particles X_1. If $n_1(i,t)$ is the number of particles X_1 inside window i at time t and $n_1(t)$ is the total number of X_1 particles on the lattice, then

$$p_i(t)=n_1(i,t)/n_1(t). \tag{6}$$

This probability set into Eq. (1) provides $S_q(t)$, the time dependent Eq. (1),

$$S_q(t)=\frac{1-\sum_{i=1}^{M} p_i^q(t)}{q-1}, \quad S_1(t)=-\sum_{i=1}^{M} p_i(t)\ln p_i(t). \tag{7}$$

For short times $S_q(t)$ scales as a nonlinear function of the time, while for large times depends nonlinearly on the system size. This nonlinear dependence on the system size is the basic indication of nonextensivity. The various values of q highlight characteristics on different length scales in the system. As an example, rare events are characterized by low values of p_i. For $q<1$, the term p_i^q takes relatively large

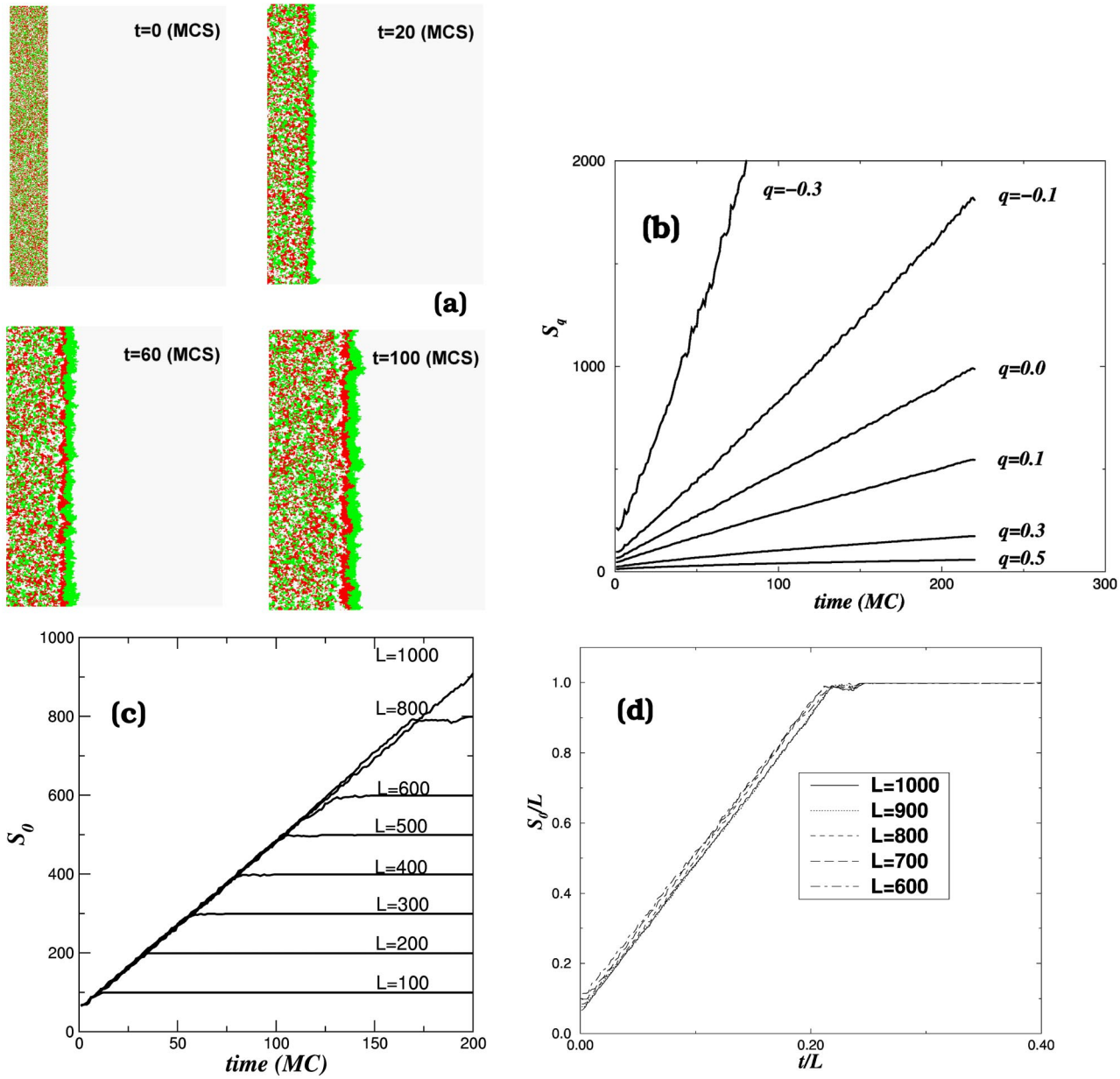

FIG. 4. (a) Four snapshots of the LLV model at the ''stripe growth'' mode; $(k_1,k_2,k_s)=(1.0,1.0,1.0)$. (b) $S_q(t)$. (c) $S_0(t)$ for $500L$ lattices. (d) Collapse of the (c) data.

values and gives important contribution to the function S_q. In contrast, if $q>1$, then $p_i^q \ll p_i$ and the contribution of rare events is negligible.

It is well known that scaling behavior is proper to systems which present fractality. Especially in monofractals only one level of scaling is detected while in multifractal structures the different scales grow with different power laws. The S_q entropy is then the appropriate measure of complexity because it addresses the complexity in different length scales by appropriate tuning of the q value.

IV. RESULTS: THE q VALUES OF ENTROPY

In the current study we explore the behavior of S_q on the LLV starting with different initial configurations. Depending on the degree of organization of the initial state, the entropy may increase going to a more disordered state or decrease going to a more ordered state.

To calculate the entropy production rate at the ''nucleus growth mode,'' we start with a fully organized state consisting only of particles S and we include a nucleation droplet of infinitesimal radius r placed on the lattice. The droplet contains particles X_1, X_2, and S homogeneously and randomly distributed within the droplet area. As time increases the droplet grows forming spontaneously several rings of particles X_1, X_2, and S sequentially [30]. The widths of the rings shrink with the distance from the pure S region and when their width becomes zero the typical LLV fractal pattern appears in the middle as can be seen in Fig. 3(a). This type of spreading is called the ''nucleus growth mode'' be-

cause an initially small droplet grows in size and finally covers the entire system. This two-dimensional ($d=2$) growth leads to a reorganization of the species which at the beginning were randomly distributed within the infinitesimal droplet, while they eventually present fractal patterns as in Fig. 2(a). As time increases this typical pattern will cover the entire lattice.

As seen in Fig. 3(b), only the case $q=0.5$ shows a *linear* increase with time during the entropy production duration; behavior is sublinear for $q>0.5$ and superlinear for $q<0.5$. In Fig. 3(c) we see $S_{0.5}$ for various system sizes. They all start linearly, coincide during the entropy production period, and saturate at different values. The q value does not change with variations of the lattice size L, of the window size l, of the initial concentrations of reactants within the original droplet, and of the values of the kinetic constants (k_1, k_2, k_3), unless the constant values or initial states drive the system to trivial states. If we inspect closely the $L=500$ steady state of Fig. 3(b), the entropy lines for $t>150$ present small fluctuations. An interesting data collapse is shown in Fig. 3(d).

In Fig. 4 the entropy of the LLV model, at the ''stripe growth mode'' is shown. This is a one-dimensional growth ($d=1$) mode. The initial state of the system consists of a stripe of randomly distributed X_1, X_2, and S embedded in a lattice containing only S particles otherwise [Fig. 4(a)]. The entropy features at this mode are similar to the nucleus growth mode but now only $q=0$ produces the linear behavior [Fig. 4(b)], hence q depends on d. Figure 4(c) shows the dependence of S_0 on the lattice size L, while the corresponding data collapse is presented in Fig. 4(d).

V. CONCLUSIONS

In the current study the nonextensive entropic properties of the LLV model are examined. The special value of q which produces a linear increase of $S_q(t)$ depends on the dimensionality d of the growth: $q=1-1/d$ $(d=1,2)$. These nontrivial values of q might be consistent with the appearance of fractal spatial structures observed in earlier studies for the same system; however, further studies are nevertheless necessary to clear out this point. Also, one expects $q=1$ in the $d\to\infty$ limit [33]. Further studies (e.g., sensitivity to the initial conditions, multifractal function $f(\alpha)$, entropy relaxation, and aging) are welcome.

ACKNOWLEDGMENTS

One of us (C.T.) acknowledges warm hospitality at the National Center for Scientific Research ''Demokritos'' and the Physics Department of the University of Athens and financial support by the General Secretariat of the Greeks Abroad, Greek Ministry of Foreign Affairs.

[1] C. Tsallis, J. Stat. Phys. **52**, 479 (1988); E.M.F. Curado and C. Tsallis, J. Phys. A **24**, L69 (1991); **24**, 3187(E) (1991); **25**, 1019(E) (1992); C. Tsallis, R.S. Mendes, and A.R. Plastino, Physica A **261**, 534 (1998).

[2] *Nonextensive Statistical Mechanics and its Applications*, edited by S. Abe and Y. Okamoto, Lecture Notes in Physics Vol. 560 (Springer-Verlag, Berlin, 2001); *Non Extensive Statistical Mechanics and Physical Applications*, edited by G. Kaniadakis, M. Lissia, and A. Rapisarda [Physica A **305** (1,2) (2002)]; *Nonextensive Entropy-Interdisciplinary Applications*, edited by M. Gell-Mann and C. Tsallis (Oxford University Press, New York, 2004); An updated bibliography can be found at the web site http://tsallis.cat.cbpf.br/biblio.htm

[3] A.R. Plastino and A. Plastino, Phys. Lett. A **174**, 384 (1993); A. R. Plastino, in *Nonextensive Statistical Mechanics and Its Applications*, edited by S. Abe and Y. Okamoto, Lecture Notes in Physics, Vol. 560 (Springer, Berlin, 2001).

[4] I. Bediaga, E.M.F. Curado, and J. Miranda, Physica A **286**, 156 (2000).

[5] C. Beck, Phys. Rev. Lett. **87**, 180601 (2001); N. Arimitsu and T. Arimitsu, Europhys. Lett. **60**, 60 (2002); M. Peyrard and I. Daumont, *ibid.* **59**, 834 (2002); A.M. Reynolds, Phys. Fluids **14**, 1442 (2002); and **15**, L1 (2003).

[6] A. Upadhyaya, J.-P. Rieu, J.A. Glazier, and Y. Sawada, Physica A **293**, 549 (2001).

[7] P.A. Alemany and D.H. Zanette, Phys. Rev. E **49**, R956 (1994); C. Tsallis, S.V.F. Levy, A.M.C. Souza, and R. Maynard, Phys. Rev. Lett. **75**, 3589 (1995).

[8] A.R. Plastino and A. Plastino, Physica A **222**, 347 (1995).

[9] M.L. Lyra and C. Tsallis, Phys. Rev. Lett. **80**, 53 (1998); U. Tirnakli, G.F.J. Ananos, and C. Tsallis, Phys. Lett. A **289**, 51 (2001); E.P. Borges, C. Tsallis, G.F.J. Ananos, and P.M.C. de Oliveira, Phys. Rev. Lett. **89**, 254103 (2002); F. Baldovin, E. Brigatti, and C. Tsallis, Phys. Lett. A **320**, 254 (2004).

[10] Y.S. Weinstein, S. Lloyd, and C. Tsallis, Phys. Rev. Lett. **89**, 214101 (2002).

[11] V. Latora, A. Rapisarda, and C. Tsallis, Phys. Rev. E **64**, 056134 (2001).

[12] L. Borland, Phys. Rev. Lett. **89**, 098701 (2002).

[13] F.A. Tamarit, S.A. Cannas, and C. Tsallis, Eur. Phys. J. B **1**, 545 (1998).

[14] S. Tong, A. Bezerianos, J. Paul, Y. Zhu, and N. Thakor, Physica A **305**, 619 (2002).

[15] A.J. Lotka, Proc. Natl. Acad. Sci. U.S.A. **6**, 410 (1920).

[16] V. Volterra, *Lecons sur la Theorie Mathematique de la Lutte pour la Vie* (Gauthier-Villars, Paris, 1936).

[17] J.D. Murray, *Mathematical Biology* (Springer-Verlag, Heidelberg, 1989).

[18] J.E. Satulovsky and T. Tome, J. Math. Biol. **35**, 344 (1997).

[19] R. Monetti, A. Rozenfeld, and E. Albano, Physica A **283**, 52 (2000).

[20] M. Droz and A. Pekalski, Physica A **298**, 545 (2001).

[21] T. Antal, M. Droz, A. Lipowski, and G. Odor, Phys. Rev. E **64**, 036118 (2001).

[22] J.E. Satulovsky, J. Theor. Biol. **183**, 381 (1996).

[23] J.E. Satulovsky and T. Tome, Phys. Rev. E **49**, 5073 (1994).

[24] B. Spagnolo, M. Cirone, A. La Barbera, and F. de Pasquale, J. Phys.: Condens. Matter **14**, 2247 (2002).
[25] A. Provata, G. Nicolis, and F. Baras, J. Chem. Phys. **110**, 8361 (1999).
[26] L. Frachebourg, P.L. Krapivsky, and E. Ben-Naim, Phys. Rev. E **54**, 6186 (1996).
[27] K. Tainaka, J. Phys. Soc. Jpn. **57**, 2588 (1988).
[28] K.I. Tainaka, Phys. Rev. Lett. **63**, 2688 (1989).
[29] G.A. Tsekouras and A. Provata, Phys. Rev. E **65**, 016204 (2002).
[30] A. Provata and G.A. Tsekouras, Phys. Rev. E **67**, 056602 (2003).
[31] G. Picard and T.W. Johnston, Phys. Rev. Lett. **48**, 1610 (1982).
[32] Y. Itoh, Prog. Theor. Phys. **78**, 507 (1987).
[33] R. Botet, M. Ploszajczak, and J.A. Gonzalez, Phys. Rev. E **65**, 015103 (2002).